Mathematical modelling of a Large-Scale Ventilated Tunnel Fire

Hui Ying WANG
Institut P', Fluides, Thermique, Combustion

CNRS-UPR3346, ENSMA, Université de Poitiers, BP 40109 F86961 Futuroscope Chasseneuil Cedex, France

1 Previous studies

In ventilated tunnel fires (cf. Fig.1), smoke and hot combustion products may form a layer near the ceiling. The pioneering theoretical work related to tunnel fire science is found by Thomas [1], on the backlayering length of hot smoke upstream the fire against a cross-stream in duct flow. By using dimensional analysis, the smoke movement has been described by Ota and Atkinson [2] and Lavid and Berlad [3] mainly from sets of equations derived by applying Froude number preservation, combined with some experimental data from a model tunnel. Atkinson and Wu [4] extended this work using the same dimensional analysis for large fires but derived corrections for slightly sloped tunnels. In order to better correlate the effects of the aspect ratio of the tunnel to the test data, Wu and Bakar [5] used hydraulic diameter instead of tunnel height in their dimensional analysis of the experimental test results. A theoretical approach for the critical velocity was adopted by Kunsch [6] through a simple analytical model to account for the physical models for a rising plume deflected at the ceiling and the integration of relevant equations for backlayering flow. Also, effort has been put into analyzing flame length, L_f, due to flame impingement in tunnel, which is the primary mode of fire spread from one object to another through radiant feedback from the hot gases. Kennedy et al. [7] have an empirical expression for the effects of wind velocity and heat release rate on the flame length, L_f. Rew and Deaves [8] presented a flame length model for tunnels, which included HRR and longitudinal velocity but not the tunnel width or height. Lönnermark and Ingason [9] show that the longitudinal ventilation shortens the flame length as the velocity increases. Fletcher et al. [10] carried out a three dimensional simulations of a full-scale mock-up of a mine roadway, as shown in Fig.1(a,b), including their experimental data. Chassé [11] simulated a naturally ventilated tunnel in two and three dimensions. Woodburn and Britter [12] indicated that the whole tunnel fire would have to be simulated, and the division of the tunnel into separate simulations was not ideal. Hwang and Edwards [13] concluded that the levelling-off of the critical ventilation velocity as the fire heat generation increases is solely due to the temperature maximum above the fire source.

Correspondence to: wang@emsma.fr

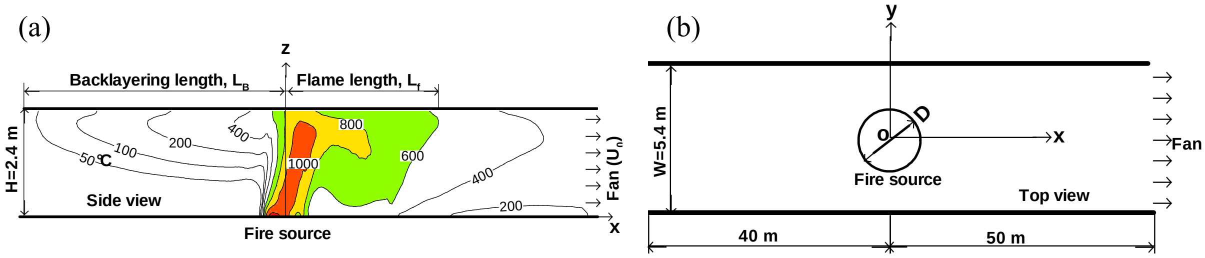

Figure 1. Full-scale tunnel fire: (a) iso-contours of the predicted temperature on the axis of symmetry of the tunnel; (b) top view of the tunnel

2 Objective of this work

In the previous works [1-13], CO and soot productions are not included, and neglect of heat transfer inside the wall results in an over-prediction of temperature. The objective of the present study is to examine the feasibility of our numerical models for understanding the effect of crossflow velocity on the local CO and soot concentrations. Influence of heat loss inside the tunnel wall on the temperature profiles is clearly shown.

3 Theoretical Analysis

Large Eddy Simulation (LES) for the fluid dynamic equations of three-dimensional elliptic, reacting flow is coupled with soot production and radiation models.

Fluid dynamic equations

Applying the filtering operation to each term in the conservation equations of mass, momentum, energy and species, and decomposing the dependent variables into resolved and subgrid components results in the filtered governing equations [14]. The perfect gas law is used to describe the equation of state.

Combustion model

The combustion model is based on the assumption that combustion is mixing-controlled via two chemical reaction steps to CO prediction [15]. The combustion processes are governed by the conservation equations for the mass fraction, Y_i, of the six major chemical species, such as C_nH_m, O_2, CO, CO_2, H_2O and N_2. The fuel oxidation can be considered as a fast reaction to CO and H_2O and the local reaction rate of fuel is calculated from an Eddy Dissipation Concept [15]. While the oxidation rate of CO is determined from both an EDC and an Arrhenius expression [16], and finally, the slowest reaction rate is taken into account.

Radiative heat transfer

In a heavily sooting flame such as fire, as the radiation spectrum of soot is continuous, it is possible to assume that the gas behaves as a gray medium. The spectral dependence is then lumped into one absorption coefficient and the radiative transfer equation without scattering is solved. The divergence of the radiative flux in the energy equation is calculated from the radiation intensity by using a discrete expression adapted to a Finite Volume Method described in Ref. [14]. The solid wall is considered as a gray diffuse one, and the boundary condition for the radiation intensity leaving a wall is determined according to the wall emissivity and its surface temperature [14]. The calculation of the gray absorption coefficients of a sooting diffusion flame is based on the work of Grosshandler (RadCal) [14].

Soot formation model

For this sooting flame, soot formation and its oxidation are incorporated into a turbulent flow calculation in two transport equations for the soot number density and soot volume fraction. The source terms include the rates of particle nucleation, soot coagulation, the surface growth of soot [17] and soot oxidation [18].

Method of resolution

Low speed solvers are used in order to explicitly eliminate compressibility effects that give rise to acoustic (sound) waves for low-Mach number flows (<0.3). While, the fluid is still considered thermally-expandable through a Boussinesq approximation. The finite-difference technique is used to discretize the partial differential equations. This procedure entails the subdividing of the calculation domain into a finite number of cells. All spatial derivatives are approximated by second-order central differences and the flow variables are updated using an explicit second-order Runge-Kutta scheme [14]. At the tunnel entrance, an open boundary condition is used, allowing combustion products to exit through the entrance if the backflow is sufficiently strong. The tunnel walls are made of concrete, and assumed to be thermally-thick, a one-dimensional heat conduction equation for the material temperature is solved.

4 Results and Discussion

This 3D tunnel geometry and the coordinate system for numerical simulation are shown in Figure 1. Airflow through the tunnel was created by the fans installed at one end by using extraction ventilation with a given volumetric flow rate. The tunnel was modelled as a rectangular prism with length L=90 m, width W=5.4 m and height H=2.4 m, with the fire source located 40 m from the entry. During the experiment, the liquid fuel, octane (C_8H_{18}), is vaporised due to flame heat feedback on the surface of the liquid fuel on a 2 cm layer of water contained in circular trays. For a pool diameter, D, of 1 m, the experimentally determined values of the fuel inflow, m_s, vary from 70, 65 to 58 g/m^{2}s as the wind velocity increases from 0.5, 0.85 to 2 m/s, providing the theoretical HRR of approximately 2-2.4 MW. In the numerical simulation, the same liquid fuel (octane) with a heat of combustion, H_c=44400 kJ/kg, is modelled, and the experimentally determined values of the fuel inflow are used. The grid system contains 250(x) x 34(y) x 48(z) cells, and at the fire source base, the length scale, Δ, determined from the cell sizes in LES, is of the order of 0.065 m. In this work, all the results from the computer outputs were time-averaged from the final 20 seconds for a 2 minutes total simulation period for comparing with the mean experimental data.

The predicted temperature profiles along the height at various locations on the axis of the tunnel downstream of the fire are compared with the experimental data in Figure 2(a,b) for the wind velocity of 0.5 m/s. With an adiabatic wall boundary condition, the computations over-predict the ceiling layer temperature by about 100 K and consequently, the vertical stratification present in the experiment. By taking into account the heat loss inside the tunnel walls which are made of concrete [10], the general behaviour of the experimentally-determined temperature field is correctly reproduced, and the difference of the maximum temperature being less than 5%. Figure 3(a,b) shows that a good agreement with the measured forward layer temperature profiles is also obtained for the wind velocities of 0.85 and 2 m/s when the heat loss inside the tunnel walls is considered.

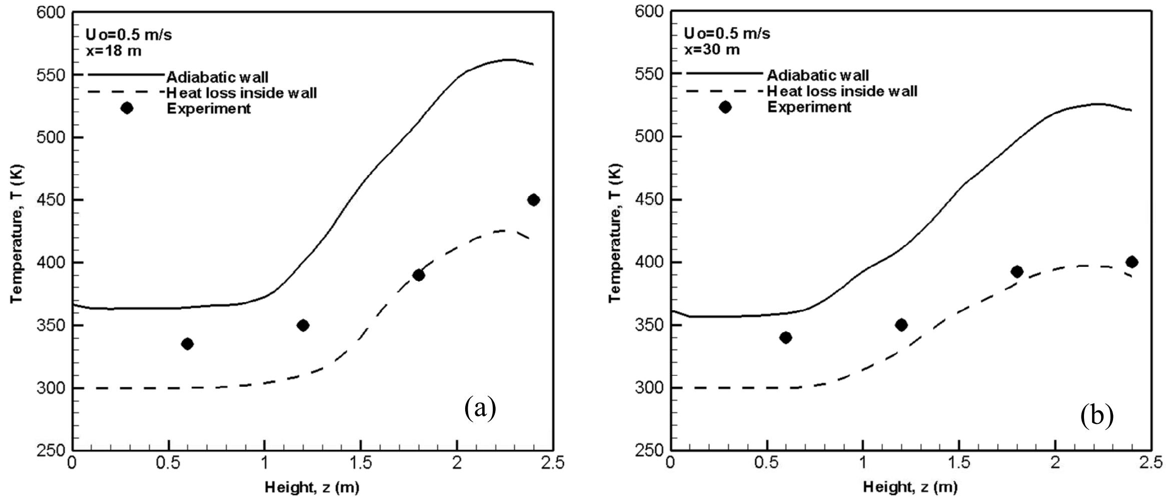

Figure 2. Comparison between the calculated and measured temperature downstream the fire under the wind velocity of 0.5 m/s: (a) x=18 m; (b) x=30 m

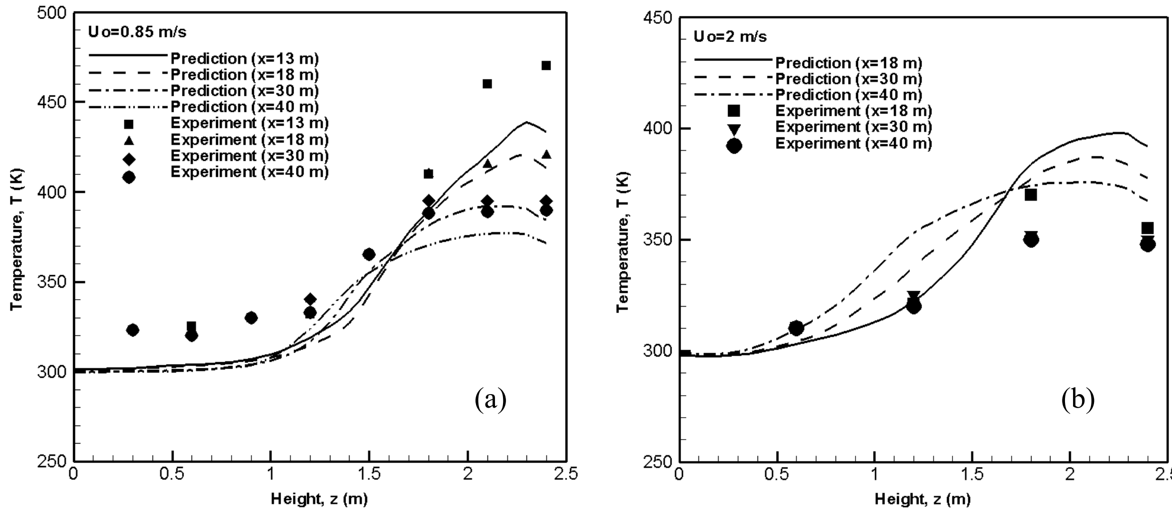

Figure 3. Comparison between the calculated and measured temperature downstream the fire with heat loss boundary condition: (a) U_o=0.85 m/s ; (b) U_o=2 m/s

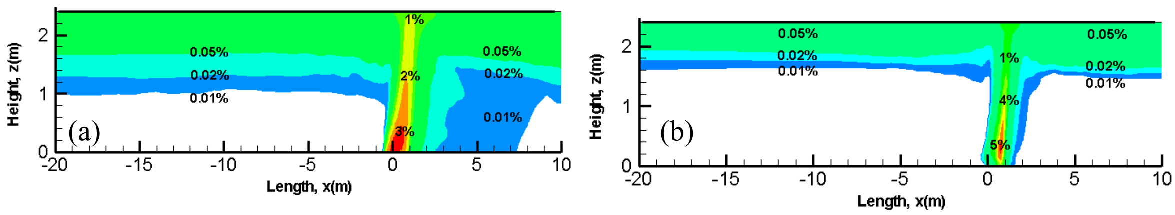

Figure 4. Iso-contours of the predicted (a) CO and (b) soot mass fractions under a wind velocity of 0.5 m/s

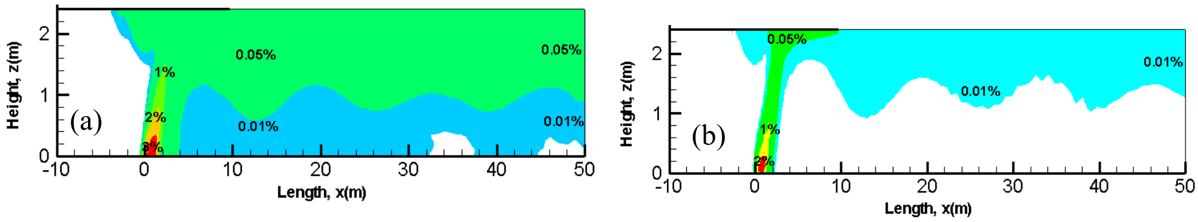

Figure 5. Iso-contours of the predicted (a) CO and (b) soot mass fractions under a critical wind velocity of 2 m/s

Iso-contours of the predicted CO and soot mass fractions on the axis of symmetry for wind velocity of 0.5 m/s are shown in Fig.4(a,b). For a fire of 2 MW, as the wind velocity is below 2 m/s, a hot smoke layer is formed near the ceiling, and progressively spreads along the ceiling against the ventilation flow through the buoyancy forces generated by the fire. The abundant CO formed around the fire base is deflected near the ceiling, and the backlayering flow brings about more toxic products up to 500 ppm with presence of a noticeable smoke stratification. It is found that the backlayering flow brings about almost the same soot quantity (mass fraction) as CO in the reverse stratified smoke layer. On the other hand, soot seems to be severely suppressed downstream the fire source at the low part of tunnel. As shown in Fig.5(a,b), a critical velocity of 2 m/s is required for a fire of 2 MW to severely suppress CO and soot upstream the fire source due to enough oxygen and turbulence development so that the fire plume tilts forward. Although, a critical ventilation helps to provide enough incoming airflow towards the channel, a high amplitude of the CO concentration up to 500 ppm is maintained all along the tunnel downstream the fire.

5 Conclusion

Validation of the numerical models was carried out for the temperature in the smoke region from a full-scale experimental tunnel fire under different ventilation rates. The present CFD results, although preliminary, indicate that heat loss within the tunnel walls has a significant effect on the temperature field near the ceiling, and consequently, on the critical velocity. When the heat loss through the tunnel walls is taken into account, the predicted results provide a good agreement in the temperature distribution as compared to the experimental data. Although, the behaviour of CO and soot production is qualitatively correct, any attempt to draw quantitative conclusions is discouraged due to uncertainties introduced by the large grid size which is primarily a problem of computational cost, and other idealizations inherent in the model.

References

[1] Thomas P. (1958). The movement of buoyant fluid against a stream and the venting of underground fire. Fire Research Station, F.R. Note No.351, Boreham Wood.

[2] Oka Y. and Atkinson G.T. (1996). Control of smoke flow in tunnel fires. Fire Saf. J. 25:305-322.

[3] Lavid M. and Berlad A.L. (1976). Gravitational effects on chemically reacting boundary layer flows over a horizontal flat plate. Proceedings of the Sixteenth Symposium (International) on Combustion. Pittsburgh : The Combustion Institute, pp.1157-67.

[4] Atkinson G.T. and Wu Y. (1996). Smoke control in sloping tunnels. Fire Saf. J. 27:335-341.

[5] Wu Y. and Bakar M.Z.A. (2000). Control of smoke flow in tunnel fires using longitudinal ventilation systems – a study of the critical velocity. Fire Saf. J. 35:363-390.

[6] Kunsch J.P. (2002). Simple model for control of fire gases in a ventilated tunnel. Fire Saf. J. 37:67-81.

[7] Kennedy W.D. (1997). Critical Velocity - Past, Present and Future (Revised 6 June 1997), presented at the American Public Transportation Association's Rail Trail Conference in Washington, DC.

[8] Rew C. and Deaves D. (1999). Fire spread and flame length in ventilated tunnels – a model used in channel tunnel assessments. Proceedings of the International Conference on Tunnel Fires and Escape from Tunnels, 397-406, Lyon, France.

[9] Lönnermark A. and Ingason H. (2006). Fire spread and flame length in large-scale tunnel fires. Fire Technology, 42(4):283-302.

[10] Fletcher D.F., Kent J.H., Apte V.B. and Green A.R. (1994). Numerical simulations of smoke movement from a pool fire in a ventilated tunnel. Fire Saf. J. 23:305-325.

[11] Chassé P. (1993). Sensitivity study of different modelling techniques for the computer simulation of tunnel fires, comparison with experimental measures. In CFDS International Users Conference. AEA Technology, UK.

[12] Woodburn P.J. and Britter R.E. (1996). CFD simulations of a tunnel fire-Part I. Fire Saf. J. 26:35-62.

[13] Hwang C.C. and Edwards J.C. (2005). The critical ventilation velocity in tunnel fires – a computer simulation. Fire Saf. J. 40:213-244.

[14] McGrattan K. (2010). Fire Dynamics Simulator – Technical Reference Guide. NIST Special Publication.

[15] Peters A.A.F. and Weber R. (1995). Mathematical modelling of a 2.25 MW swirling natural gas flame. Part 1: eddy break-up concept for turbulent combustion; probability density function approach for nitric oxide formation. Combust. Sci. and Tech. 110:67-101.

[16] Dryer F.L. and Glassman I. High-temperature oxidation of CO and CH_4. Proceedings of the 14th Symposium (International) on Combustion. Pittsburgh : The Combustion Institute, pp.987-1003.

[17] Moss J.B., Stewart C.D. and Young K.J. (1995). Modelling soot formation and burnout in a high temperature laminar diffusion flame burning under oxygen-enriched conditions. Combust Flame, 101:491-500.

[18] Nagle J. and Strickland-Constable R.F. (1962). Oxidation of carbon between 1000-2000°C. Proceedings of 5th Conference on Carbon, Vol.1, pp. 154-164.